

# Computational study of cycloaddition reactions on the SiC(1 0 0)-c(2 × 2) surface

V.M. Bermudez \*

Naval Research Laboratory, 4555 Overlook Ave., S.W., Washington, DC 20375-5347, USA

Received 12 December 2002; accepted for publication 19 May 2003

## Abstract

Cycloaddition reactions between 1,3-butadiene and the C-terminated SiC(1 0 0)-c(2 × 2) surface have been addressed using quantum-chemical methods. The c(2 × 2) structure consists of  $\text{—C}\equiv\text{C—}$  bridges between underlayer Si atoms which themselves form Si—Si bonds. Of various possible reaction products, the one formed by a [2 + 4] reaction with the  $\text{—C}\equiv\text{C—}$  bridge (giving a species resembling 1,4-cyclohexadiene) is the lowest in energy. Density functional calculations for the bare c(2 × 2) surface, using a cluster model with mechanical embedding, gave good agreement with structural parameters obtained in previous fully ab initio studies. Similar calculations for the cycloaddition product and for the transition state gave a reaction energy of  $-50.3$  kcal/mol and an activation energy of  $+6.1$  kcal/mol to form a planar ring structure lying normal to the surface. Detailed results for the frequency and infrared polarization behavior of adsorbate vibrational modes have also been obtained.

© 2003 Elsevier B.V. All rights reserved.

**Keywords:** Models of surface chemical reactions; Chemisorption; Silicon carbide; Alkenes

## 1. Introduction

Cycloaddition reactions of alkenes and dienes with weakly  $\pi$ -bonded dimers on the (1 0 0)-(2 × 1) surfaces of the column-IV semiconductors C (diamond), Si and Ge have received much attention [1–3]. Such reactions provide an important class of methods for fabricating “functionalized” semiconductor surfaces with potential applications in chemical sensors and in hybrid electronic devices. Ab initio quantum-chemical modeling [4–12] has

been a powerful tool in understanding structure and reactivity in these cycloaddition processes.

In this work, we consider cycloaddition reactions between 1,3-butadiene (the prototypical diene) and the (1 0 0) surface of the IV–IV compound semiconductor cubic SiC. The SiC(1 0 0) surface exhibits several reconstructions, depending on stoichiometry, which have been reviewed recently from both experimental [13,14] and theoretical [15] perspectives. Here we focus on the very unusual C-terminated c(2 × 2) structure consisting (see below) of essentially *triple-bonded*  $\text{—C}\equiv\text{C—}$  bridges between Si atoms which themselves form Si—Si  $\sigma$ -bonds. The resulting surface has no dangling bonds and no intrinsic surface states in the band gap. Previous theoretical studies [16,17] have addressed

\* Fax: +1-202-767-1165.

E-mail address: [bermudez@estd.nrl.navy.mil](mailto:bermudez@estd.nrl.navy.mil) (V.M. Bermudez).

the chemisorption of small molecules on SiC(100) surfaces; although, to our knowledge, the particular behavior of the  $c(2 \times 2)$  in this regard has been largely unexplored.

## 2. Results and discussion

### 2.1. Possible adsorbate structures

Fig. 1 shows a schematic diagram of the SiC(100)- $c(2 \times 2)$  surface. Fig. 2 illustrates six different adsorbate structures which could, *hypothetically*, be formed by reaction with 1,3-butadiene. The bare  $c(2 \times 2)$  surface will be examined in detail below.

The first step was to evaluate the relative energies of the various adsorbate structures. This was done by constructing the cluster model for the bare  $c(2 \times 2)$  shown in Fig. 3a and using either a semiempirical or a molecular mechanics (MM) approach to optimize the geometries of the

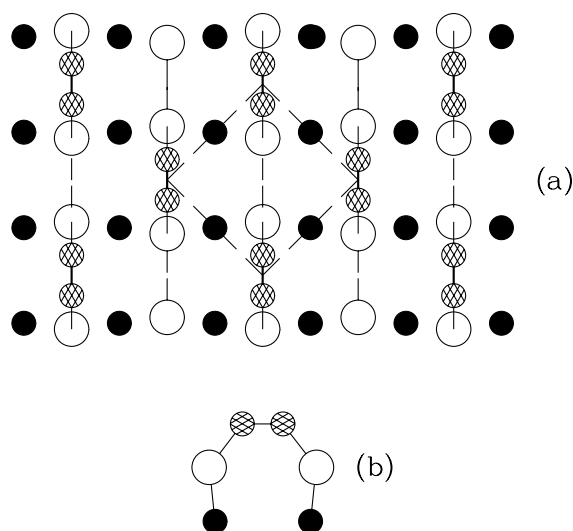


Fig. 1. Schematic model for the SiC(100)- $c(2 \times 2)$  surface [13,15] viewed along the surface normal (a) and in the surface plane (b). The cross-hatched circles are the  $\text{—C}\equiv\text{C—}$  bridges lying above the plane. The open circles are the first-underlayer Si atoms lying in the plane, and the filled circles are the second-underlayer C atoms lying below the plane. Dashed lines show the bonds between Si atoms, and the dashed square shows the  $c(2 \times 2)$  surface unit cell.

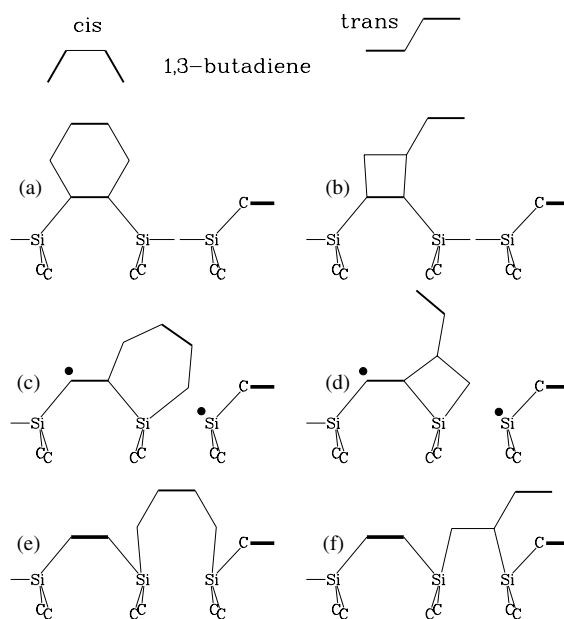


Fig. 2. Schematic models for the six possible 1,3-butadiene reaction products considered in the present work. The *cis* and *trans* molecular structures are also shown. The small filled circles in (c) and (d) indicate unpaired electrons. Heavy lines indicate  $>\text{C}=\text{C}<$   $\pi$ -bonds, and extra-heavy lines show  $\text{—C}\equiv\text{C—}$   $\pi$ -bonds. Dashed lines show Si—Si  $\sigma$ -bonds. For clarity the H atoms and most of the C atoms are not shown explicitly. The structures are idealized models and have not been optimized.

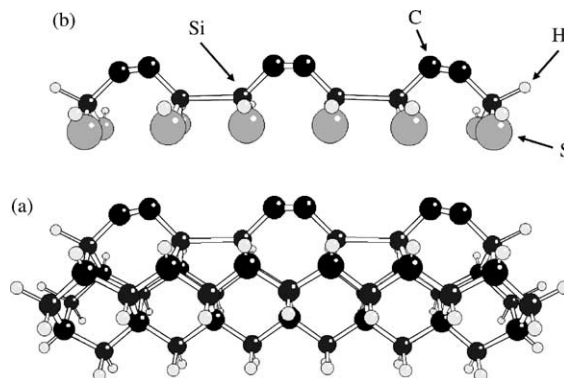


Fig. 3. Schematic diagram of the cluster model for the  $c(2 \times 2)$  surface. (a) shows the entire  $\text{Si}_{26}\text{C}_{25}\text{H}_{46}$  cluster, and (b) shows the “high-level” part treated via DFT. The remainder of (a) forms the “low-level” part treated using RHF/PM3 or UFF methods. The various atom types, including the S link atoms, are indicated. The structure shown is the result of the geometry optimization.

cluster + adsorbate (bonded as in Fig. 2). For the former, restricted Hartree Fock (RHF) calculations were done at the PM3 level [18]. Badziag [19] has performed a purely semiempirical treatment of the bare  $c(2 \times 2)$  surface at the RHF/PM3 level, using a periodic cluster model, and obtained good agreement with *ab initio* geometries (see below). For MM, the Universal Force Field (UFF) [20] in the Gaussian98 program suite [21] was used.

Structures based on reaction across the Si—C bond (Fig. 2c, d) are unfavorable because they result in unpairing of electrons in the  $-\text{C}\equiv\text{C}-$  and Si—Si bonds of the bare surface. These were not further considered in the present calculations. Of the remaining four structures, both methods (RHF/PM3 and UFF) agree that the product formed by [2 + 4] cycloaddition at the  $-\text{C}\equiv\text{C}-$  bridge (Fig. 2a) is the most stable. The RHF/PM3 result places this at  $\sim 38$  kcal/mol below the second-most stable structure, the [2 + 2] product (Fig. 2b). A more accurate value for this energy difference is given below. The prediction of the [2 + 4] (vs. [2 + 2]) cycloaddition product as being the more stable is consistent with *ab initio* results for the reaction of 1,3-butadiene with the (1 0 0)- $(2 \times 1)$  surfaces<sup>1</sup> of C [4], Si [5,8] and Ge [8]. It is also noted that the [2 + 2] reaction is symmetry-forbidden, according to the Woodward-Hoffman rules, for a symmetric  $-\text{C}\equiv\text{C}-$  bridge as in Fig. 1b. However, on the real surface (see below) the bridge is asymmetric, which makes the [2 + 2] formally allowed (although still energetically unfavorable). In the following, attention will focus mainly on the [2 + 4] reaction, with some further mention of the [2 + 2].

## 2.2. The bare $c(2 \times 2)$ surface

A cluster model was constructed for the bare  $c(2 \times 2)$  surface as a basis for treating the adsorbate. This was done using a mechanical-embedding (ME) approach [22], as implemented in the Gaussian98 program suite [21], which has been applied successfully to surface problems [23]. The

ME technique used was that recently developed by Krüger and Sax [24] involving divalent atoms (Be, O or S), rather than H, as link atoms. (Link atoms replace cluster atoms during the high-level treatment of the chemically-significant sub-section of the cluster.) Fig. 3a shows the entire cluster, and Fig. 3b shows the part that was treated at the high level, together with the S link atoms. The surface Si—Si bonds are an integral part of the  $c(2 \times 2)$  structure, and this sub-cluster is the smallest that can possibly be expected to include these adequately. Forming the high-level sub-section requires breaking two Si—C bonds. Initial attempts to use H as the link atom, which then gives two Si—H bonds per high-level Si atom, led to difficulties in geometry optimization which were eliminated by the present approach.

The low-level part of the ME calculation was done using either RHF/PM3 or UFF methods. The UFF atom types [20] were declared to be “H\_” and “Si3” for H and Si, “C\_3” and “C\_1”, respectively, for sub-surface C and  $-\text{C}\equiv\text{C}-$  and “S\_2” for the S link atoms. The high-level treatment of the sub-cluster (Fig. 3b) was done using density functional theory (DFT) with the B3LYP functional, and no constraints were applied in the geometry optimization. In the following, calculations will be termed “(A/B:C)” where “A” is the high-level method (usually B3LYP), “B” the high-level basis set (usually 6-31G\*) and “C” the low-level method (either PM3, meaning RHF/PM3, or UFF).

Table 1 (cf. Fig. 4a) compares structural results with those obtained using fully *ab initio* slab-model treatments [25–28] and with the available experimental data [29–31]. In the following, only the central  $-\text{C}\equiv\text{C}-$  bridge will be considered, in order to avoid ambiguities due to edge effects. All calculations give a  $-\text{C}\equiv\text{C}-$  distance of about 1.21 Å, close to the corresponding value [32] in the molecule  $\text{H}_3\text{SiC}\equiv\text{CSiH}_3$  (1.216 Å). The Si—Si distance found in previous, fully *ab initio* work [25–28] is close to that for dimers on the Si(1 0 0)- $(2 \times 1)\text{H}$  monohydride surface (2.39 Å [5]). In either system, there are no unpaired dangling orbitals on surface Si atoms. The (B3LYP/6-31G\*:PM3) value obtained here ( $d_3 = 2.42$  Å) is in good agreement with these results. The (B3LYP/

<sup>1</sup> The Ge results in [8] are for Ge—Ge dimers on a Si(1 0 0) surface.

Table 1  
Structural results for the ME cluster model (“this work”) vs. fully ab initio treatments of the SiC(100)-c(2×2) surface

Distance	Yan [25]	Käckell [26]	Sabisch [27]	Catellani [28]	This work <sup>a</sup>	Expt.
$d_1$	1.22	1.23	1.22	1.23	1.23 (1.23)	1.22 <sup>b</sup> 1.31 <sup>c</sup>
$d_2$	1.87	1.82	1.83	1.81	1.85 (1.84)	1.84 <sup>b</sup> 1.93 <sup>c</sup>
$d_3$	2.38	2.38	2.40	2.37	2.42 (2.53)	2.70 <sup>b</sup> 2.71 <sup>c</sup>
$\delta z_1$	1.30	1.32	1.32		1.32 (1.30)	1.60 <sup>c</sup>
$\delta z_2$	1.02		1.04		1.08 (1.12)	1.07 <sup>c</sup>

All distances are in Ångstroms. The terms are defined in Fig. 4a.

<sup>a</sup> Values given are the (B3LYP/6-31G\*:PM3) results. Those in parentheses are from the (B3LYP/6-31G\*:UFF) calculation.

<sup>b</sup> Photoelectron diffraction data [29,30] for a sample prepared by thermal desorption of Si from a Si-terminated surface.

<sup>c</sup> Low energy electron diffraction data [31] for a sample prepared by desorption of Si. Surfaces prepared by exposure to C<sub>2</sub>H<sub>4</sub> at high temperature gave somewhat different distances, possibly due to the presence of adsorbed H.

6-31G\*:UFF) result, while somewhat greater ( $d_3 = 2.53$  Å), is still much less than the Si–Si distance on the ideally-terminated SiC(100) surface, 3.08 Å. Thus, the ME treatment of the cluster shown in Fig. 3 appears to be comparable to fully ab initio models in describing  $\text{—C}\equiv\text{C—}$  bridges on the c(2×2) surface. None of the results, including those obtained here, show the experimentally-observed tilting (“buckling”) of the  $\text{—C}\equiv\text{C—}$  bridge [33,34]. Recent work [35] indicates that the tilting may be due to stress along the  $\text{—C}\equiv\text{C—}$  bridge, which was not considered in the models included in Table 1. Also, the calculated Si–Si distance ( $d_3$ ) is, in all cases, significantly shorter than the experimental value.

Unrestricted (UB3LYP) calculations were done to test for the possibility that the Si–Si bond might be so weak that unpaired spin density would appear on surface Si atoms. However, the calculation always converged to a closed-shell singlet. The vibrational frequencies of the optimized structure were checked for the absence of imaginary values which would indicate a geometric instability. Of the possible divalent link atoms Be, O and S [24], preliminary (UHF/3-21G:UFF) calculations found that only S gave good convergence in geometry optimization. The optimized geometry was remarkably insensitive to the choice of high-level method and basis set. A comparison of (UHF/3-21G:UFF) and (B3LYP/6-31G\*:UFF) results showed differences in  $d_1$ ,  $d_2$  and  $d_3$  of 2% and in  $\delta z_1$  ( $\delta z_2$ ) of 3% (7%). Table 1 also shows

that, except as noted above, the structure is essentially independent of the low-level method.

### 2.3. The [2 + 4] cycloaddition product: structure and reaction energy

The cluster model was augmented to include the [2 + 4] product at the central  $\text{—C}\equiv\text{C—}$  bridge (Fig. 4b), and Table 2 gives the optimized structural parameters. The adsorbate resembles 1,4-cyclohexadiene (Fig. 4c) with the plane of the six-member ring lying normal to the surface. Both theoretical [36] and spectroscopic [37] results indicate that the free 1,4-cyclohexadiene ring is planar, and the same was found here for the cycloaddition product. The absence of imaginary vibrational frequencies indicates that this is a stable structure. The  $d_1$  and  $d_6$  distances are typical of a C=C  $\pi$ -bond, and the  $d_4$  and  $d_5$  values are typical of a C–C  $\sigma$ -bond. The C–H distances are 1.088 Å for C=C–H and 1.103 Å for CH<sub>2</sub>. These values and  $d_5$  and  $d_6$  are all close (within  $\sim 0.01$  Å) to the corresponding values reported in a recent theoretical study of molecular 1,4-cyclohexadiene [36]. Distances involving only substrate atoms (i.e.,  $d_3$  and  $\delta z_2$ ) are essentially unaffected by adsorption (compare corresponding methods in Tables 1 and 2). This suggests that underlayer atoms, particularly the Si–Si bond, are not strongly involved in chemisorption at the  $\text{—C}\equiv\text{C—}$  site and supports the use of the small sub-cluster (Fig. 3b).

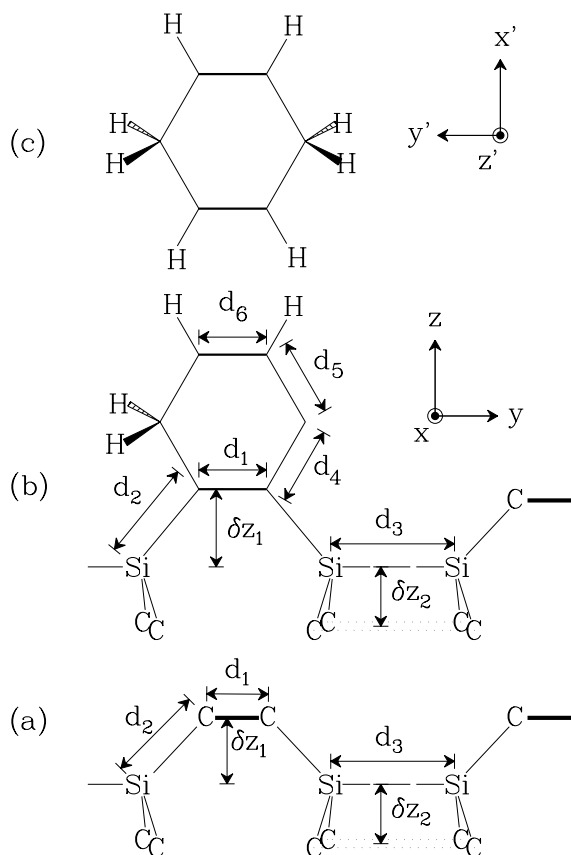


Fig. 4. (a) Schematic diagram showing the distances (cf. Table 1) defining the  $c(2 \times 2)$  surface structure. The extra-heavy C—C lines indicate the  $\text{—C}\equiv\text{C—}$   $\pi$ -bonds. (b) Schematic diagram of the  $[2 + 4]$  cycloaddition reaction product for 1,3-butadiene and the  $c(2 \times 2)$  surface (cf. Table 2). The heavy lines indicate  $\text{>C=C<}$   $\pi$ -bonds. For clarity, the ring C atoms and the two H atoms on one of the C atoms are omitted. (c) The free 1,4-cyclohexadiene molecule. The different coordinate systems for the symmetry analysis of (b) and (c) are indicated.

To obtain a value for the energy of reaction ( $\Delta E_R$ ), defined as the energy difference between the product and the reagents at 0 K, similar calculations were done for free 1,3-butadiene. Table 3 compares the result,  $\Delta E_R = -54.8$  eV, with those for the same reaction on other surfaces. For the present results, the electronic energies were corrected for the zero-point (ZP) vibrational energies, and the *cis* form of 1,3-butadiene was used as the reagent (as required by the geometry of the  $[2 + 4]$  product). The *trans* form was computed to be lower in energy by 3.5 kcal/mol; hence,  $\Delta E_R$  would

Table 2  
Structural parameters (Å), defined in Fig. 4b, for the reaction product and for the transition state

Distance	Product	Transition state
$d_1$	1.36 (1.36)	(1.26)
$d_2$	1.92 (1.91)	(1.84)
$d_3$	2.49 (2.55)	(2.54)
$d_4$	1.53 (1.53)	(2.43)
$d_5$	1.50 (1.50)	(1.37)
$d_6$	1.33 (1.33)	(1.43)
$\delta z_1$	1.57 (1.55)	(1.35)
$\delta z_2$	1.06 (1.11)	(1.12)

Values in parentheses are from (B3LYP/6-31G\*:UFF) calculations. The others are (B3LYP/6-31G\*:PM3) results.

be less exothermic by this amount if the *trans* form were used as the reagent. It is likely that strain makes a significant contribution to  $\Delta E_R$ . For the bare  $c(2 \times 2)$  surface the computed Si—C≡C angle is  $135^\circ$ , far removed from the ideal  $sp$ -hybridized value of  $180^\circ$ ; whereas, in the reaction product the Si—C=C angle is  $126^\circ$ , close to the ideal  $sp^2$  value of  $120^\circ$ .

Some of the  $\Delta E_R$  values in Table 3 are for different basis sets, but the differences for the various semiconductors are greater than the expected basis-set dependencies. For example,  $\Delta E_R$  for the  $[2 + 4]$  cycloaddition reaction of 1,3-cyclohexadiene with Si(100)-(2 × 1) [5] is <3% more exothermic for 6-311G\*\* than for 6-31G\* basis sets. In the present case, the basis-set dependence was examined using single-point (B3LYP/6-311+G\*:PM3) calculations for structures optimized at the (B3LYP/6-31G\*:PM3) level. The ZP corrections at the (B3LYP/6-31G\*:PM3) level were also used. The result is  $\Delta E_R = -50.3$  kcal/mol, ~8% less exothermic than the all-(B3LYP/6-31G\*:PM3) result. It is speculated that the larger basis-set dependence in this case may indicate that including a diffuse function improves the description of the weak (i.e., long) Si—Si bond. With B3LYP/6-31G\* as the high-level method, little or no difference is noted between results obtained with RHF/PM3 or UFF as the low-level method. This will be useful in treating the transition state (see below).

Similar calculations were also performed for the  $[2 + 2]$  reaction product. The ZP-corrected (B3LYP/6-31G\*:PM3) result places this species

Table 3

Comparison of reaction ( $\Delta E_R$ ) and activation ( $\Delta E_A$ ) energies computed for the [2+4] cycloaddition reaction of 1,3-butadiene with various surfaces

Substrate	$\Delta E_R$	$\Delta E_A$
C(100)-(2×1)	-76.2 <sup>a</sup>	+5.2
	-84.3 to -85.5 <sup>b</sup>	+2.7 to +1.9
Si(100)-(2×1)	-67.5 <sup>c</sup>	
	-61.8 <sup>d</sup>	
Ge(100)-(2×1) <sup>e</sup>	-45.8 <sup>d</sup>	
SiC(100)-c(2×2)	-54.8 (-56.4) <sup>f</sup>	(+4.7)
	-50.3 <sup>g</sup>	(+6.1)

All values are in kcal/mol, and negative values indicate an exothermic process. All studies used DFT with the B3LYP functional. The footnotes give the basis sets, the form ("cis" or "trans") of 1,3-butadiene used as the reagent (see text), and whether it was explicitly stated that electronic energies were corrected for zero-point (ZP) vibrational energy.

<sup>a</sup> Ref. [4] (6-31+G\*; cis; ZP-corrected).

<sup>b</sup> Ref. [11] (6-31G\*; cis; ZP-corrected). Results depend slightly on cluster size.

<sup>c</sup> Ref. [5] (6-31G\*; cis).

<sup>d</sup> Ref. [8] (6-31G\* for terminating H and bulk Si, 6-311+G\*\* for surface Si or Ge and for 1,3-butadiene; trans).

<sup>e</sup> These results are for Ge-Ge dimers on a Si(100) surface.

<sup>f</sup> Present work [(B3LYP/6-31G\*:PM3); cis; ZP-corrected]. Values in parentheses are (B3LYP/6-31G\*:UFF) results. The trans form of 1,3-butadiene was computed to lie 3.5 kcal/mol (ZP-corrected) lower than the cis at the B3LYP/6-31G\* level.

<sup>g</sup>  $\Delta E_R$  as in f but for (B3LYP/6-311+G\*:PM3) single-point calculations using the (B3LYP/6-31G\*:PM3) structures and ZP-corrections obtained in f. The  $\Delta E_A$  value (in parentheses) is the (B3LYP/6-311+G\*:UFF) single-point result obtained using the (B3LYP/6-31G\*:UFF) transition state structures and ZP-corrections in f.

23.5 kcal/mol above the [2+4] product. The present result is close to the [2+2]–[2+4] difference computed for 1,3-butadiene reacting with Si and diamond (100)-(2×1). For Si, values (not cis–trans corrected) of 25.6 [5] and 24.8 kcal/mol [8] have been found. For diamond, a value of 28.2 kcal/mol [4] has been reported. For both Si(100) [38] and C(100) [4], analysis of infrared (IR) spectroscopic data indicates that the reaction is predominantly [2+4], and the same is expected for SiC(100)-c(2×2).

#### 2.4. Vibrational spectra

The frequencies of adsorbate vibrational modes are compared in Table 4 with corresponding values from IR [39,40] and Raman [37] data for liquid 1,4-cyclohexadiene. The calculated modes are all localized within the adsorbate; although, those below  $\sim 1100$   $\text{cm}^{-1}$  exhibit small contributions from other atoms. Hence, the frequencies are accurate at the B3LYP/6-31G\* level [22] and have been scaled accordingly [41]. Some free-molecule modes will of course be strongly perturbed in the adsorbate. Results for RHF/PM3 or UFF (not

shown) as the low-level method differed by  $\leq 4$   $\text{cm}^{-1}$  except for the stretching mode of the C=C bonded to Si (1561  $\text{cm}^{-1}$  in Table 4) which was 25  $\text{cm}^{-1}$  lower for UFF. Vibrational modes were also obtained for the [2+2] product but are not given here.

The relevant surface experiment [1] is typically done using IR spectroscopy in the multiple internal reflection (MIR) configuration<sup>2</sup> which provides polarization data. In principle, high-resolution electron energy loss spectroscopy could also be used. However, for a partially ionic material such as SiC, detection of weak adsorbate modes is complicated by the presence of strong Fuchs-Kliwer phonon losses [42].

Issues related to symmetry are now considered. The point-group of the free, planar 1,4-cyclohexadiene molecule is  $D_{2h}$ , and that of the adsorbate (Fig. 4b) is  $C_{2v}$  with (x,z) and (y,z) as mirror

<sup>2</sup> Only adsorbate modes calculated to lie above 1000  $\text{cm}^{-1}$  are given in Table 4. For an MIR experiment using as a sample a thin film of SiC grown on a Si substrate, this would be the approximate lower limit of the accessible range imposed by the transmission of the Si MIR element.

Table 4

Computed vibrational frequencies ( $\text{cm}^{-1}$ ) for the cycloaddition product (“adsorbate”) together with corresponding IR and Raman values for liquid 1,4-cyclohexadiene

Mode <sup>a</sup>	Adsorbate <sup>b</sup>	IR [39] <sup>c</sup>	Raman [37]
=CH sym. str. <sup>d</sup>	3061 (z;100)		3031 ( $A_g$ , $B_{2g}$ ) <sup>e</sup>
=CH asym. str. <sup>d</sup>	3040 (y;12)	3019 ( $B_{1u}$ , $B_{3u}$ ) <sup>e</sup> ; vvs	
CH <sub>2</sub> asym. str.	2875 (forb.)		2866 ( $B_{3g}$ )
CH <sub>2</sub> asym. str.	2874 (x;44)	2877 ( $B_{2u}$ ); vvs	
CH <sub>2</sub> sym. str.	2868 (z;8)		2884 ( $A_g$ ) <sup>f</sup>
CH <sub>2</sub> sym. str.	2868 (y;8)	2825 ( $B_{1u}$ ); vvs	
C=C sym. str. <sup>g</sup>	1694 (z;7)		1680 ( $A_g$ )
C=C asym. str. <sup>g</sup>	1561 (z;5)	1639 ( $B_{3u}$ ); vvs	
CH <sub>2</sub> scissor	1435 (y;15)	1430 ( $B_{1u}$ ); vvs	
CH <sub>2</sub> scissor	1430 (z;2)		1428 ( $A_g$ )
HC=CH i-p bend <sup>d</sup>		1405 ( $B_{1u}$ ); vs	
HC=CH i-p bend <sup>d</sup>	1377 (y;1)		1378 ( $B_{2g}$ )
CH <sub>2</sub> wag	1326 (z;3)	1358 ( $B_{3u}$ ); m	
CH <sub>2</sub> wag	1336 (y;6)		1280 ( $B_{2g}$ ) <sup>h</sup>
CH <sub>2</sub> twist	1202 (forb.)	1249 ( $A_u$ ) <sup>h</sup>	
CH <sub>2</sub> twist	1197 (x;1)		1242 ( $B_{1g}$ ) <sup>h</sup>
HC=CH i-p bend <sup>d</sup>	1164 (z;0)		1200 ( $A_g$ )
HC=CH i-p bend <sup>d</sup>		1159 ( $B_{3u}$ ); m	
“ring stretch” <sup>g</sup>	1050 (y;19)		1038 ( $B_{2g}$ )
“ring stretch” <sup>g</sup>	980 (y;11)	887 ( $B_{1u}$ )	

Calculated frequencies are (B3LYP/6-31G\*:PM3) results, scaled by a factor of 0.9613 (Ref. [41]). Only calculated modes above  $\sim 1000 \text{ cm}^{-1}$  are given. For IR and Raman data, symmetry assignments for the  $D_{2h}$  point group are given.

<sup>a</sup> str. = stretch; sym. = symmetric (i.e., in-phase); asym. = antisymmetric (i.e., out-of-phase); i-p = in-plane. The mode descriptions (“sym. str.”, etc.) are those given in [37,40] for the free molecule.

<sup>b</sup> Calculated (this work). “x”, “y” and “z” indicate polarization behavior in IR absorption (axes defined in Fig. 4b). “Forb.” indicates “IR-forbidden” for  $C_{2v}$  symmetry. The number following the polarization label is the computed relative intensity on a scale of 0–100.

<sup>c</sup> Relative intensities [39] are indicated qualitatively: vvs = very very strong; vs = very strong; m = moderately strong.

<sup>d</sup> There is only one H—C=C—H group in the adsorbate; hence, only one mode remains from each pair of modes in the free molecule.

<sup>e</sup> These modes are accidentally degenerate in the free molecule.

<sup>f</sup> This mode is believed to be shifted to higher energy by a Fermi resonance [40] with the overtone of the CH<sub>2</sub> scissor mode.

<sup>g</sup> In the adsorbate, the two C=C bonds are no longer equivalent. The higher- (lower-) energy C=C stretching mode involves mainly the H—C=C—H (Si—C=C—Si) group. For the same reason, the “ring-stretching” modes differ from those of the free molecule.

<sup>h</sup> These are estimated frequencies [40]. The  $A_u$  modes are IR- and Raman-forbidden in the  $D_{2h}$  point group. The other estimates are for modes which, although allowed, are too weak to be observed.

planes and  $z$  as the twofold rotation axis.<sup>3</sup> Upon reduction from  $D_{2h}$  to  $C_{2v}$ , all modes become IR-allowed except those belonging to the  $B_{3g}$  and  $A_u$  representations of  $D_{2h}$ . These correlate [43] with the  $A_2$  representation of  $C_{2v}$  which is IR-forbidden. The  $A_g$  and  $B_{3u}$  modes of the free molecule (which correlate with  $A_1$  of  $C_{2v}$ ) are allowed in  $z$ -polarization. The  $B_{1g}$  and  $B_{2u}$  modes (which correlate with  $B_1$  of  $C_{2v}$ ) are allowed in  $x$ -polarization.

The  $B_{2g}$  and  $B_{1u}$  modes (which correlate with  $B_2$  of  $C_{2v}$ ) are allowed in  $y$ -polarization. If the experiment is done on a two-domain surface, with equal numbers of rings lying in the  $(x, z)$  and  $(y, z)$  planes, no distinction can be made between  $x$ - and  $y$ -polarized modes. Of course, a polarized MIR experiment on a single-domain sample would provide more detailed data. Such a single-domain  $c(2 \times 2)$  structure has been used previously in surface-sensitive, polarized  $x$ -ray absorption experiments [44].

In Table 4, the polarization of each calculated mode was determined by examining the atomic

<sup>3</sup> In the convention used here, the  $x'$ -axis of  $D_{2h}$  is preserved as the twofold rotation axis upon reduction to  $C_{2v}$ .

displacements and applying the  $C_{2v}$  symmetry operations. The polarization assignments were thus determined independently of the  $D_{2h} \leftrightarrow C_{2v}$  correlations given above. The results show that of all the adsorbate modes above  $1000\text{ cm}^{-1}$  only two are  $x$ -polarized. In addition to the adsorbate vibrations, the calculation gave a  $\text{—C}\equiv\text{C—}$  stretching mode at  $2028\text{ cm}^{-1}$  on the bare surface which is allowed in  $z$ -polarization, given the  $C_{2v}$  symmetry of the  $c(2\times 2)$  surface unit cell (Fig. 1). The absorption is predicted to be relatively strong (48 on the scale of Table 4) and is comparable in frequency to the corresponding mode ( $2132\text{ cm}^{-1}$  [45]) in the Raman spectrum of liquid  $\text{H}_3\text{SiC}\equiv\text{CSiH}_3$ . The removal of this mode upon adsorption on the  $c(2\times 2)$  surface may be detectable in an MIR experiment, and observation of such a high-frequency stretching vibration would be further proof of the triple-bond nature of the  $\text{—C}\equiv\text{C—}$  bridge.

### 2.5. The transition state

Fig. 5 shows an energy-level diagram, following Okamoto [11], which compares the  $[2+4]$  cycloaddition reaction of 1,3-butadiene with molecular  $\text{C}_2\text{H}_2$  and with the  $\text{—C}\equiv\text{C—}$  bridge on the  $c(2\times 2)$  surface. The energies of the molecular HOMOs were obtained from photoemission data [46] and the HOMO–LUMO separations from B3LYP/6-31G\* calculations for the respective free molecules. The experimental [46] 1,3-butadiene HOMO en-

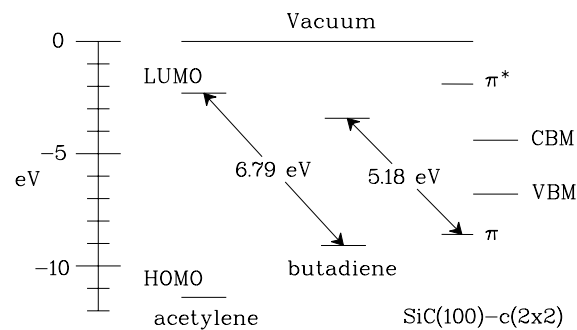


Fig. 5. Schematic energy level diagram showing the alignment of the 1,3-butadiene HOMO and LUMO with those of free acetylene ( $\text{C}_2\text{H}_2$ ) and with the  $\text{—C}\equiv\text{C—}$   $\pi$  and  $\pi^*$  orbitals on the  $\text{SiC}(100)\text{—}c(2\times 2)$  surface.

ergy is that of the stable *trans* form. The position of the  $\text{SiC}$  conduction band minimum (CBM) below vacuum is given by the measured [47] electron affinity for the  $c(2\times 2)$  surface, 4.4 eV. The valence band maximum (VBM) lies lower than the CBM by the cubic  $\text{SiC}$  band gap energy [48] of 2.40 eV. The positions of the  $\text{—C}\equiv\text{C—}$   $\pi$  and  $\pi^*$  states relative to the VBM and CBM were obtained from the theoretical results of Sabisch et al. [27].

For  $\text{C}_2\text{H}_2$ , the large energy difference between the LUMO of the “dienophile” ( $\text{C}_2\text{H}_2$ ) and the HOMO of the diene means that the reaction will be slow under normal conditions. In fact, it has been observed only in the presence of metal catalysts [49,50]. However, the dienophile HOMO on the  $c(2\times 2)$  surface is at a much higher energy than in free  $\text{C}_2\text{H}_2$  which reduces the energy difference for the so-called “reverse-electron-demand” reaction, in analogy with the  $\text{C}(100)\text{—}(2\times 1)$  surface [11]. The energy difference of 5.18 eV (Fig. 5) is somewhat greater than the corresponding value of 4.60 eV computed [11] for this reaction on the  $\text{C}(100)\text{—}(2\times 1)$  surface modeled as a  $\text{C}_9\text{H}_{12}$  cluster.

Fig. 6 shows the transition state obtained in a QST3 optimization [21]. Because of the computational effort involved, only (B3LYP/6-31G\*:UFF) calculations were done. A UB3LYP calculation showed no unpaired spin density and gave the same optimized energy. As noted above, the results are expected to be essentially the same as those obtained with RHF/PM3 as the low-level method. The appearance of a single imaginary frequency shows that the structure corresponds to a first-order saddle point. Bond lengths, defined as in Fig. 4b, are given in Table 2. Of most interest are  $d_4 = 2.43\text{ \AA}$  (the length of the bond forming between surface and adsorbate C atoms) and the angle of  $\phi = 51.8^\circ$  between the 1,3-butadiene plane and the surface normal (cf. Fig. 6b). These are similar to the corresponding values of 2.64–2.68  $\text{\AA}$  [4,11] and  $49^\circ$  [4] for  $\text{C}(100)\text{—}(2\times 1)$ .

The activation energy,  $\Delta E_A = +6.1\text{ kcal/mol}$ , is somewhat greater than for the same reaction on  $\text{C}(100)\text{—}(2\times 1)$  [4,11]. It is useful at this point to consider whether it is reasonable to expect the reaction studied here to occur under conditions accessible in a typical ultra-high vacuum (UHV) chamber. Experimentally, the  $\text{C}(100)\text{—}(2\times 1)$  re-



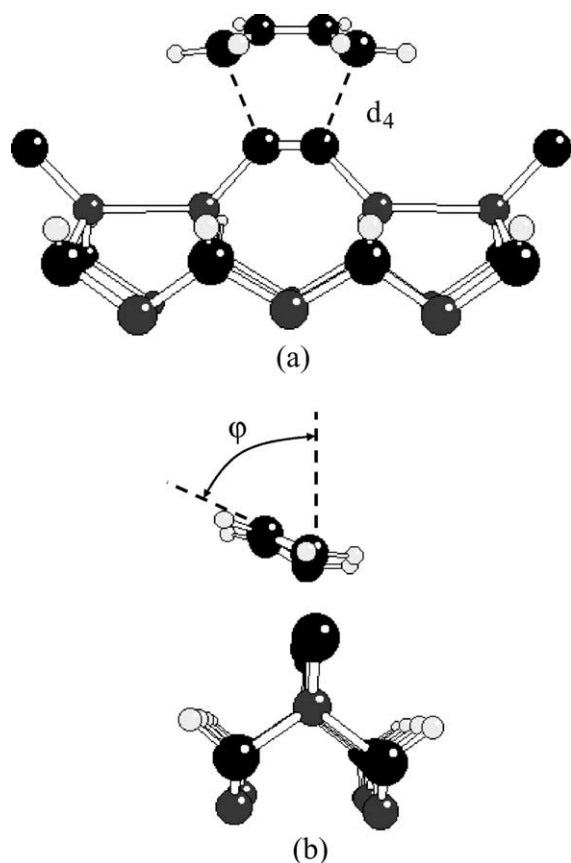


Fig. 6. Schematic diagram showing part of the cluster, together with 1,3-butadiene, in the transition-state configuration. (a) and (b) are viewed along the  $x$ - and  $y$ -axes respectively (cf. Fig. 4b).

action is found [51–53] to be facile at room temperature, and chemisorption saturates at a 1,3-butadiene exposure of  $\sim 30$  L (1 Langmuir (L)  $\equiv 10^{-6}$  Torr s) [54]. Assuming similar pre-exponential factors for the two systems,  $\Delta E_A \approx 3$  kcal/mol for C(100)-(2x1) and  $\sim 6$  kcal/mol for SiC(100)-c(2x2), as in Table 3, suggests that the reaction will be slower by a factor of  $\sim 150$  for the c(2x2) at room temperature. The required exposure of  $\sim 5 \times 10^3$  L for SiC(100)-c(2x2) is certainly feasible in a UHV system for a simple hydrocarbon like 1,3-butadiene. This is especially true in an IR spectroscopy or scanning tunneling microscopy experiment, for which it is unnecessary to re-evacuate all the way back to UHV conditions after exposure in order to record data.

### 3. Summary and conclusions

The reaction of 1,3-butadiene with SiC(100)-c(2x2) surface has been considered using computational methods. The results are as follows:

- (1) Semiempirical and MM calculations predict that the [2+4] cycloaddition product with the  $-\text{C}\equiv\text{C}-$  bridge is the most stable of six hypothetical adsorbate structures.
- (2) A cluster model for the bare c(2x2) surface was constructed using ME with divalent link atoms [24]. A hybrid calculation with B3LYP/6-31G\* as the high-level method and either semiempirical (RHF/PM3) or MM (UFF) methods in the low-level gave an optimized structure that compares well with previous, fully ab initio results.
- (3) The cycloaddition product was treated by including the 1,3-butadiene adsorbate in the high-level section. For the [2+4] reaction, the resulting structure resembles 1,4-cyclohexadiene. A reaction energy of  $\Delta E_R = -50.3$  kcal/mol, with an activation energy of  $\Delta E_A = +6.1$  kcal/mol, was obtained. The corresponding [2+2] reaction product was found to lie 23.5 kcal/mol higher in energy.
- (4) The vibrational spectrum of the adsorbate was analyzed. Normal-mode frequencies, absorption intensities and polarization effects expected in IR spectroscopy were described.

### Acknowledgements

This work was supported by the Office of Naval Research and by a grant of computer time from the DOD High Performance Computing Modernization Program at the ASC-MSRC, Wright-Patterson AFB. J. Hess (Gaussian, Inc.) is thanked for consultation and assistance. B.I. Dunlap is thanked for helpful discussions and for a critical reading of the manuscript.

### References

- [1] S.F. Bent, J. Phys. Chem. B 106 (2002) 2830.

- [2] R.J. Hamers, S.K. Coulter, M.D. Ellison, J.S. Hovis, D.F. Padowitz, M.P. Schwartz, C.M. Greenlief, J.N. Russell Jr., *Acc. Chem. Res.* 33 (2000) 617.
- [3] R.A. Wolkow, *Annu. Rev. Phys. Chem.* 50 (1999) 413.
- [4] D.R. Fitzgerald, D.J. Doren, *J. Am. Chem. Soc.* 122 (2000) 12334.
- [5] R. Konečný, D.J. Doren, *Surf. Sci.* 417 (1998) 169.
- [6] R. Konečný, D.J. Doren, *J. Am. Chem. Soc.* 119 (1997) 11098.
- [7] G.T. Wang, C. Mui, C.B. Musgrave, S.F. Bent, *J. Phys. Chem. B* 103 (1999) 6803.
- [8] C. Mui, S.F. Bent, C.B. Musgrave, *J. Phys. Chem. A* 104 (2000) 2457.
- [9] X. Lu, X. Xu, N. Wang, Q. Zhang, M.C. Lin, *J. Phys. Chem. B* 105 (2001) 10069.
- [10] C.H. Choi, M.S. Gordon, *J. Am. Chem. Soc.* 121 (1999) 11311.
- [11] Y. Okamoto, *J. Phys. Chem. B* 105 (2001) 1813.
- [12] J.-H. Cho, D.-H. Oh, K.S. Kim, L. Kleinman, *J. Chem. Phys.* 116 (2002) 3800.
- [13] V.Yu. Aristov, *Physics – Uspekhi* 44 (2001) 761.
- [14] P. Soukiassian, *Mater. Sci. Eng. B* 96 (2002) 115.
- [15] A. Catellani, G. Galli, *Progr. Surf. Sci.* 69 (2002) 101.
- [16] A.J. Dyson, P.V. Smith, *Surf. Sci.* 396 (1998) 24.
- [17] J. Olander, K. Larsson, *J. Phys. Chem. B* 103 (1999) 9604.
- [18] J.J.P. Stewart, *J. Comput.-Aided Mol. Design* 4 (1990) 1.
- [19] P. Badziag, *Phys. Rev. B* 44 (1991) 11143.
- [20] A.K. Rappé, C.J. Casewit, K.S. Colwell, W.A. Goddard III, W.M. Skiff, *J. Am. Chem. Soc.* 114 (1992) 10024.
- [21] M.J. Frisch et al., *Gaussian 98, Revision A. 11*, Gaussian, Inc., Pittsburgh, PA, 2001.
- [22] S. Dapprich, I. Komáromi, K.S. Byun, K. Morokuma, M.J. Frisch, *J. Mol. Struct. (Theochem)* 461–462 (1999) 1.
- [23] N. Lopez, G. Pacchioni, F. Maseras, F. Illas, *Chem. Phys. Lett.* 294 (1998) 611.
- [24] T. Krüger, A.F. Sax, *J. Comput. Chem.* 23 (2002) 371.
- [25] H. Yan, A.P. Smith, H. Jónsson, *Surf. Sci.* 330 (1995) 265.
- [26] P. Käckell, J. Furthmüller, F. Bechstedt, G. Kresse, J. Hafner, *Phys. Rev. B* 54 (1996) 10304.
- [27] M. Sabisch, P. Krüger, A. Mazur, M. Rohlfing, J. Pollmann, *Phys. Rev. B* 53 (1996) 13121.
- [28] A. Catellani, G. Galli, F. Gygi, *Phys. Rev. Lett.* 77 (1996) 5090.
- [29] M. Shimomura, H.W. Yeom, B.S. Mun, C.S. Fadley, S. Hara, S. Yoshida, S. Kono, *Surf. Sci.* 438 (1999) 237.
- [30] H.W. Yeom, M. Shimomura, J. Kitamura, S. Hara, K. Tono, I. Matsuda, B.S. Mun, W.A.R. Huff, S. Kono, T. Ohta, S. Yoshida, H. Okushi, K. Kajimura, C.S. Fadley, *Phys. Rev. Lett.* 83 (1999) 1640.
- [31] J.M. Powers, A. Wander, P.J. Rous, M.A. Van Hove, G.A. Somorjai, *Phys. Rev. B* 44 (1991) 11159.
- [32] S. Cradock, K.A.S. Nicoll, D.W.H. Rankin, *J. Mol. Struct. Sci.* 216 (1990) 213.
- [33] V. Derycke, P. Soukiassian, A. Mayne, G. Dujardin, *Surf. Sci.* 446 (2000) L101.
- [34] B. Stankiewicz, L. Jurczyszyn, *Surf. Sci.* 507–510 (2002) 463.
- [35] F.-H. Wang, P. Krüger, J. Pollmann, *Phys. Rev. B* 66 (2002) 195335.
- [36] M. Merchán, L. Serrano-Andrés, L.S. Slater, B.O. Roos, R. McDiarmid, X. Xing, *J. Phys. Chem. A* 103 (1999) 5468.
- [37] H. Hagemann, H. Bill, D. Joly, P. Müller, N. Pautex, *Spectrochim. Acta* 41 (1985) 751.
- [38] A.V. Teplyakov, M.J. Kong, S.F. Bent, *J. Chem. Phys.* 108 (1998) 4599.
- [39] H.D. Stidham, *Spectrochim. Acta* 21 (1965) 23.
- [40] O. Ermer, S. Lifson, *J. Mol. Spectrosc.* 51 (1974) 261.
- [41] M.W. Wong, *Chem. Phys. Lett.* 256 (1996) 391.
- [42] H. Nienhaus, V. van Elsbergen, W. Mönch, *Eur. Phys. J. B* 9 (1999) 179.
- [43] S. Califano, *Vibrational States*, Wiley, New York, 1976.
- [44] J.P. Long, V.M. Bermudez, D.E. Ramaker, *Phys. Rev. Lett.* 76 (1996) 991.
- [45] R.C. Lord, D.W. Mayo, H.E. Opitz, J.S. Peake, *Spectrochim. Acta* 12 (1958) 147.
- [46] K. Kimura, S. Katsumata, Y. Achiba, T. Yamazaki, S. Iwata, *Handbook of Hel Photoelectron Spectra of Fundamental Organic Molecules*, Japan Scientific Societies Press, Tokyo, 1981.
- [47] F.S. Tautz, S. Sloboshanin, S. Hohenecker, D.R.T. Zahn, J.A. Schaefer, *Appl. Surf. Sci.* 123/124 (1998) 17.
- [48] G.L. Harris (Ed.), *Properties of Silicon Carbide*, IEEE-INSPEC, London, 1995.
- [49] R. Bakhtiar, J.J. Drader, D.B. Jacobson, *J. Am. Chem. Soc.* 114 (1992) 8304.
- [50] K. Schroeter, C.A. Schalley, R. Wesendrup, D. Schröder, H. Schwarz, *Organometallics* 16 (1997) 986.
- [51] M.Z. Hossain, T. Aruga, N. Takagi, T. Tsuno, N. Fujimori, T. Ando, M. Nishijima, *Jpn. J. Appl. Phys.* 38 (1999) L1496.
- [52] G.T. Wang, S.F. Bent, J.N. Russell Jr., J.E. Butler, M.P. D'Evelyn, *J. Am. Chem. Soc.* 122 (2000) 744.
- [53] J.N. Russell Jr., J.E. Butler, G.T. Wang, S.F. Bent, J.S. Hovis, R.J. Hamers, M.P. D'Evelyn, *Mater. Chem. Phys.* 72 (2001) 147.
- [54] J.N. Russell Jr., personal communication.